ARTICLES

Mechanism of DNA translocation in a replicative hexameric helicase

Eric J. Enemark[1] & Leemor Joshua-Tor[1]

The E1 protein of papillomavirus is a hexameric ring helicase belonging to the AAA+ family. The mechanism that couples the ATP cycle to DNA translocation has been unclear. Here we present the crystal structure of the E1 hexamer with single-stranded DNA discretely bound within the hexamer channel and nucleotides at the subunit interfaces. This structure demonstrates that only one strand of DNA passes through the hexamer channel and that the DNA-binding hairpins of each subunit form a spiral 'staircase' that sequentially tracks the oligonucleotide backbone. Consecutively grouped ATP, ADP and apo configurations correlate with the height of the hairpin, suggesting a straightforward DNA translocation mechanism. Each subunit sequentially progresses through ATP, ADP and apo states while the associated DNA-binding hairpin travels from the top staircase position to the bottom, escorting one nucleotide of single-stranded DNA through the channel. These events permute sequentially around the ring from one subunit to the next.

Replication initiation only occurs at specific DNA sites (origin of replication, *ori*), and can only occur once per cell division. Initiation begins with binding of *ori* by an origin-recognition protein such as bacterial DnaA (reviewed in ref. 1) or yeast ORC (reviewed in ref. 2). Subsequently, a helicase is assembled at *ori* and DNA polymerase(s), primase(s) and other factors are recruited to form the replisome, which processively synthesizes DNA complementarily to the template. In eukaryotes replication initiation involves many proteins. Even in *Escherichia coli*, at least three proteins (DnaA, DnaB and DnaC)[1] are required just to establish the replicative helicase at *ori*. Small DNA viruses such as papillomavirus, SV40 and AAV (adeno-associated virus) use a single initiator protein for origin recognition, helicase loading and helicase activity itself.

The viral initiator proteins E1, large T-antigen and Rep (from papillomavirus, SV40 and AAV, respectively) belong to helicase superfamily III (SF3; reviewed in ref. 3) and are members of the AAA+ (ATPases associated with cellular activities) family[4]. These helicases form hexameric rings that are believed to encircle substrate DNA and unwind it with $3' \rightarrow 5'$ polarity[5–7]. These properties resemble those of bacteriophage T7 gene product 4 (T7gp4) and *E. coli* DnaB, two hexameric replicative helicases that exhibit the opposite $5' \rightarrow 3'$ polarity[8,9]. Both T7gp4 and DnaB have been shown to encircle only one of the two DNA strands[10,11]. The strand displacement assays used to determine the polarity of SF3 helicases indicates that the hexamers will load upon a single-stranded $3'$ tail[7,12], suggesting that the ring encircles this strand while sterically excluding the other. A mechanism where double-stranded DNA (dsDNA) passes through the channel after assembly at the *ori* was proposed for these helicases[13,14]. However, the crystal structures of SV40 T-antigen (Tag)[13,14] demonstrate channel diameters of <7 Å in the ATP-bound state and $\sim$15 Å in the apo state in the AAA+ domains; this is insufficient to permit the passage of $\sim$20-Å-diameter dsDNA, suggesting that only ssDNA can be accommodated.

Papillomavirus and SV40 have a closed circular genome, and consequently no ends are available for loading an intact ring. Whereas most DNA helicases require a region of ssDNA for entry, E1 and Tag can initiate unwinding from completely dsDNA, apparently by causing helix melting and entry of the DNA helicase onto a single-stranded region. Sequence similarity between the carboxy-terminal halves of E1 and SV40 T-antigen, which contain the AAA+ domain, is significant. The amino-terminal halves of the proteins, which contain the DNA-binding domain (DBD), share little sequence similarity, but their structures are highly similar[15,16], reinforcing the likelihood that they use analogous mechanisms. The closed ring topology of their genomes suggests that the helicase is loaded as an open ring[17], as proposed for DNA processivity clamps[18], or as monomers sequentially until a hexameric ring encircling the DNA is produced[17,19]. E1 carries out its transition from site-specific dsDNA binding (origin binding activity) to aspecific single-stranded binding and unwinding (helicase activity) via a transition of stoichiometry from a dimer to a double hexamer through a series of discrete intermediate oligomeric states assembled directly upon progressively distorted[6,19–21] and ultimately melted origin DNA[22,23]. To determine the topological and atomic details of DNA coordination by this group of ring helicases, and to elucidate features of the DNA translocation mechanism, we have determined the crystal structure of a bovine papillomavirus (BPV) E1 fragment comprising the AAA+ and oligomerization domains in complex with ssDNA, ADP and Mg^{2+}.

Overall architecture

The crystal consists of two hexamers (subunits A–F for hexamer 1 and G–L for hexamer 2), each encircling a single strand of DNA (Fig. 1). The six oligomerization domains form a rigid collar with near proper six-fold rotational symmetry. The arrangement of the AAA+ domains resembles the arrangement in the Tag hexamer[14] and in the predicted human papillomavirus type 18 (HPV-18) E1 AAA+ domain hexamer[24]. However, unlike the oligomerization domains, in this case they deviate significantly from proper six-fold symmetry. Most of the protein–DNA interactions occur at hairpins located at the interior of the channel, which narrows to $\sim$13 Å in diameter. These hairpins resemble a spiral staircase as they sequentially track the sugar-phosphate backbone of the ssDNA in a right-handed helical arrangement of a consistent set of interactions (Fig. 2). The

[1]W. M. Keck Structural Biology Laboratory, Cold Spring Harbor Laboratory, 1 Bungtown Road, Cold Spring Harbor, New York 11724, USA.

subunits have varying modes of Mg^{2+}–ADP coordination, and each P-loop appears to have an associated ADP molecule except for subunit L.

DNA binding

All of the residues observed to interact with ssDNA are located at the interior of the hexameric ring on the AAA+ domains (Fig. 2). The K506 ammonium group interacts with one ssDNA phosphate oxygen while the H507 main-chain amide proton forms a hydrogen bond with the ssDNA phosphate of an adjacent nucleotide. The aliphatic portion of K506 and the aromatic groups of F464 and H507 form van der Waals interactions with the ssDNA sugar moiety linking these two phosphates. This set of interactions permutes sequentially around the hexameric ring with concurrent unitary ssDNA nucleotide progression between the subunits. The 5′ end of the ssDNA is directed towards the N-terminal oligomerization domains, whereas the 3′ end is directed towards the C terminus. The protein–DNA interactions are consistent between the two hexamers with one notable exception. One hexamer has five of the subunit hairpins engaged in ssDNA phosphate coordination whereas the other hexamer engages all six subunit hairpins. The details of this difference illustrate a logical transition within a cyclic translocation mechanism described below.

Intersubunit interactions and ADP binding

The most robust intersubunit interactions occur between the oligomerization domains through consistent interactions at each interface. The interactions between the AAA+ domains either mediate nucleotide binding or are involved in 'staircasing' the hairpins. As with Tag, the RFC (replication factor C) clamp loader, and other multisubunit AAA+ protein complexes, the amino acids responsible for nucleotide coordination and hydrolysis are located on adjacent subunits. One contains the Walker A, Walker B and sensor-1 motifs. The adjacent subunit provides additional elements such as the arginine finger. For the E1–DNA hexamer, the intersubunit arrangement and separation varies. Consequently, the atomic details of nucleotide binding vary between the subunits (Fig. 3). In all cases, the Walker A and B motifs are consistently structured and generally coordinate the diphosphate group of an ADP molecule and an associated Mg^{2+} ion. In contrast, the adjacent subunit has three fundamental forms that correlate with the 'order' travelling around the ring as well as the vertical position of the DNA-binding hairpin in the staircase.

Form I is present at three of the interfaces in hexamer 1 and at two of the interfaces in hexamer 2 (see also Supplementary Fig. S1 and Supplementary Table S1). This form involves an intricate network of interactions between adjacent subunits (Fig. 3). Based on three factors, this form of nucleotide coordination is classified as ATP-type: (1) simultaneous engagement of all the AAA+ components implicated in ATP coordination and hydrolysis; (2) all of these elements structurally align with equivalents in the $(Tag\text{-}ATP)_6$ structure (Supplementary Fig. S2); and (3) a chloride ion sits at the anticipated position for an ATP γ-phosphate in three of the five cases (difference density is also observed at 2.5σ and 3σ in the other two cases but has not been modelled). The positions of K425 and R538 (the arginine finger) are major factors that define this nucleotide coordination mode. The ammonium group of K425 concurrently binds the α- and β-phosphate in a position very similar to the sensor-2 arginine, R217, of RuvB, an AAA+ protein involved in Holliday branch migration. As a result, we classify this lysine as 'sensor-2'. The arginine finger, R538, simultaneously binds a Walker B aspartate of the first subunit, D479, and a water molecule that coordinates the Mg^{2+} ion. Notably, the guanidinium group of R538

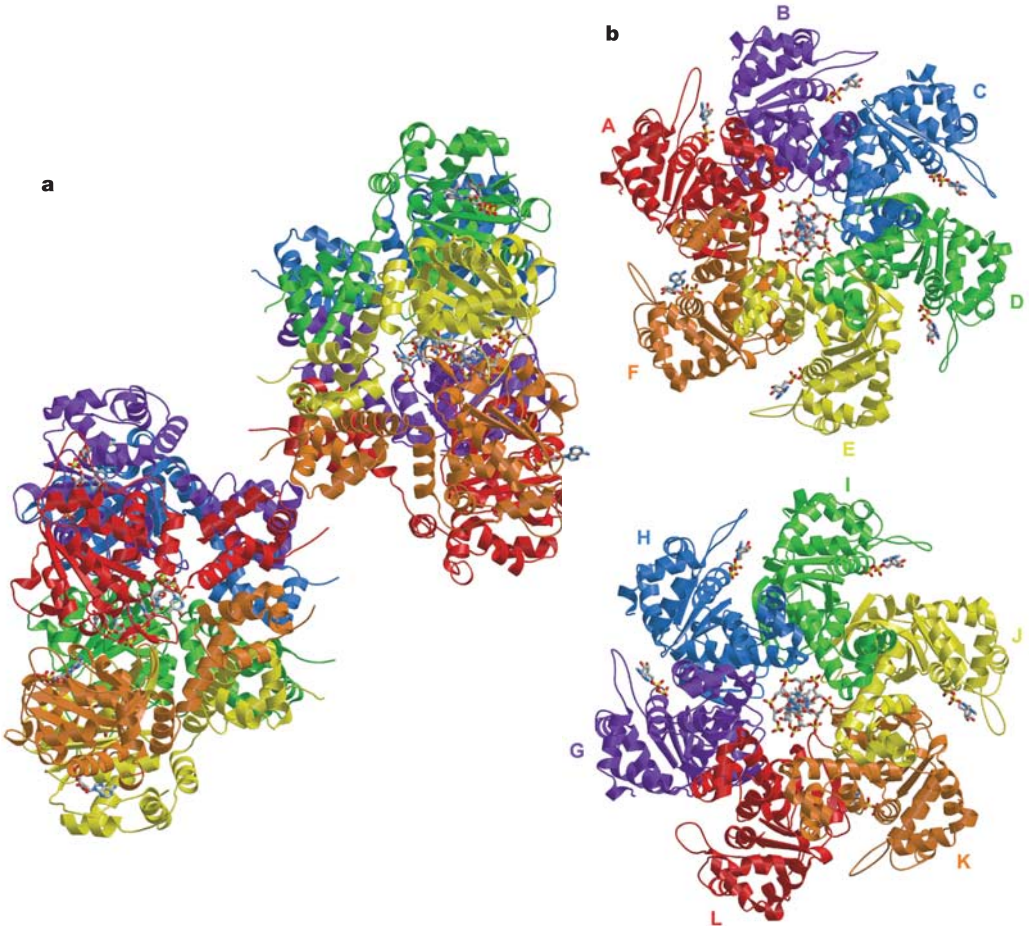

Figure 1 | Structure of the E1 hexameric helicase in complex with ssDNA and ADP. **a**, **b**, Ribbon representations of the two E1 helicase hexamers viewed perpendicular (**a**) and parallel (**b**) to the channels. Individual subunits are colour-coded with hexamer 1 on top and hexamer 2 on the bottom. A crystal lattice interaction between the hexamers is illustrated (**a**). The oligomerization domains form a rigid collar, located between the AAA+ domains in **a** and projected towards the reader in **b**. The DNA in the central channel and the ADP molecules at subunit interfaces are depicted in stick representation. Images were prepared with Bobscript[34] and Raster3D[35,36].

is appropriately positioned to interact with the γ-phosphate of an ATP, generally occupied by a Cl^- ion in the crystal structure. The Cl^- ion also interacts with sensor-1 of the first subunit, N523. Several residues on a connected pair of helices participate in this coordination. Arginine R493, denoted here as 'sensor-3', interacts with D489 as well as the Walker B aspartate, D479, and sensor-1, N523. Tyrosine Y499 interacts with the ADP α-PO_4.

Form II uses the Walker A and B motifs of one subunit, but only Y499 of the adjacent subunit (Fig. 3). In this form, most of the ATP-type interactions are absent and display flexibility. R493 interacts with Walker B D479 and sensor 1 N523 of the neighbouring subunit for the interface between subunits D and E of hexamer 1 and the I–J interface of hexamer 2. However, it is too distant for the E–F (hexamer 1) and J–K (hexamer 2) interfaces (see also Supplementary Fig. S1). A striking difference between this form and the ATP type described above is the sandwiching of Y534 between R493 and R538 (arginine finger). This interaction places R538 too distant to interact with a γ-PO_4 of an ATP molecule. The greatly reduced interactions and complete exclusion of the arginine finger led us to classify this as 'ADP-type' coordination. No Cl^- ions are observed in this form.

Form III does not use any residues of the adjacent subunit and also binds the Mg^{2+} ion differently than the preceding forms (Fig. 3). This form has been classified as 'apo' due to the total lack of involvement of the adjacent subunit. In the apo-type coordination, an ADP molecule is usually present at the Walker A and B motif regions, but it is coordinated differently than above. In the K–L interface, the α-PO_4 and β-PO_4 of the ADP molecule adopt a reverse orientation relative to the other subunit interfaces.

Correlation of nucleotide state with hairpin height

The DNA-binding hairpins form a right-handed staircase that sequentially tracks the ssDNA backbone. The vertical position on the staircase for the hairpin of a given subunit correlates with the type of nucleotide coordination. The subunits that participate in ATP-type coordinations place their hairpins at the top of the staircase; the hairpins of apo-type subunits occupy the bottom of the staircase. The hairpins of ADP-type subunits lie at the intermediate positions. The staircase is maintained by a consistent set of interactions (Fig. 2) between the hairpins of adjacent subunits involving K506, which also contacts a ssDNA phosphate as described above. The ammonium group of this lysine interacts with three sites on the adjacent hairpin: the acidic group of D504 and the main-chain carbonyl groups of R505 and K508. These staircasing elements are conserved in all E1 sequences as well as in Tag and AAV, and we expect these proteins to exhibit the same sets of interactions and form a staircase of hairpins when ssDNA and multiple nucleotide states are present simultaneously (Supplementary Fig. S3). Previous crystal structures of Tag, which lacked DNA and possessed a single nucleotide state[13,14], did not display a staircase of hairpins. Interestingly, a hexameric ring structure of T7gp4, which had multiple nucleotide states but lacked DNA[25], also demonstrated a staircase of the DNA-binding hairpins via a lysine (K467, chain C) and an acidic residue (D470, chain B). These interactions were maintained between subunits with assigned ATP-type coordination. Also, these staircasing elements appear to be conserved in DnaB, as shown from a sequence alignment with T7gp4 (Supplementary Fig. S4). The adoption of a staircase by DNA-binding hairpins through a set of interactions involving a

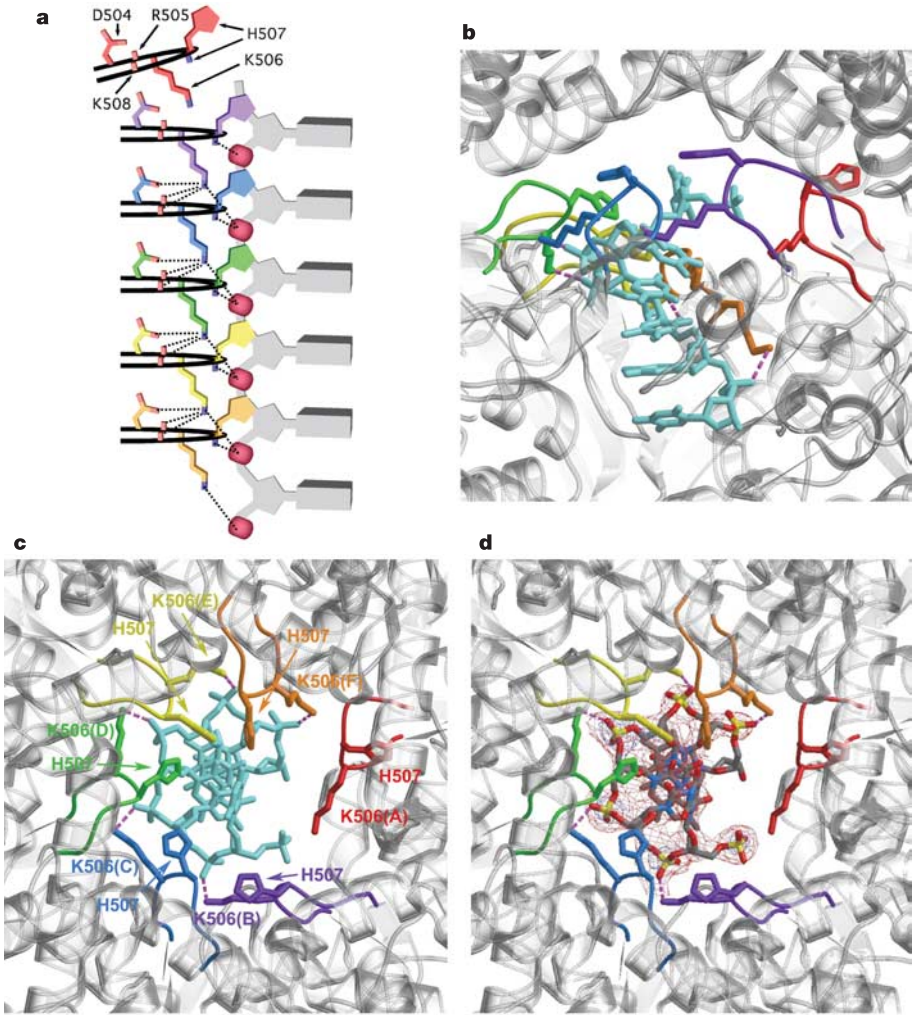

Figure 2 | DNA binding in the E1 hexameric helicase. **a**–**c**, Interactions involving the AAA+ hairpins and ssDNA shown as a schematic (**a**) and as a ribbon diagram in two perpendicular views (**b**, **c**) for hexamer 1. K506 coordinates a ssDNA phosphate, and the main-chain amide of H507 interacts with the phosphate of an adjacent nucleotide. K506 also mediates interactions with three sites on the adjacent hairpin to form the staircase of hairpins—the side chain of D504 and the main chain carbonyl groups of R505 and K508 (the latter two side chains are omitted for clarity). Hydrogen bonds are drawn as dotted (**a**) or dashed (**b**–**d**) lines. Hairpins of the individual subunits are colour-coded as in Fig. 1. In **b** and **c** only H507 and K506 side chains are shown. The letters in parentheses identify the subunits. Other components of the protein are coloured grey with transparency. The DNA is in light blue. **d**, Same as **c** with superimposed $F_o - F_c$ difference electron density calculated before inclusion of any DNA in the model. The electron density is contoured at 3σ (red) and at 6σ (blue).

basic and an acidic residue of a neighbouring subunit may be a fundamental feature of hexameric helicases.

The correlation of nucleotide state with vertical position of the DNA-binding hairpins is consistent with previous structural observations for Tag in the absence of DNA[13,14]. Apart from the presence of DNA, the major difference here is that these states are all present in the same hexamer.

The crystal structure of hexameric T7gp4 bound to the non-hydrolysable ATP analogue ADPNP in the absence of DNA also exhibits multiple nucleotide-binding configurations with an associated trend for the DNA-binding loops[25]. A crystallographic two-fold-related set of three sites is observed, two with associated ADPNP molecules (ATP-type and ADP-type) and one empty.

A coordinated escort mechanism for DNA translocation

The hexameric structures determined here display varying nucleotide coordination modes that correlate with the vertical position of the associated DNA-binding hairpins. The ssDNA nucleotides are

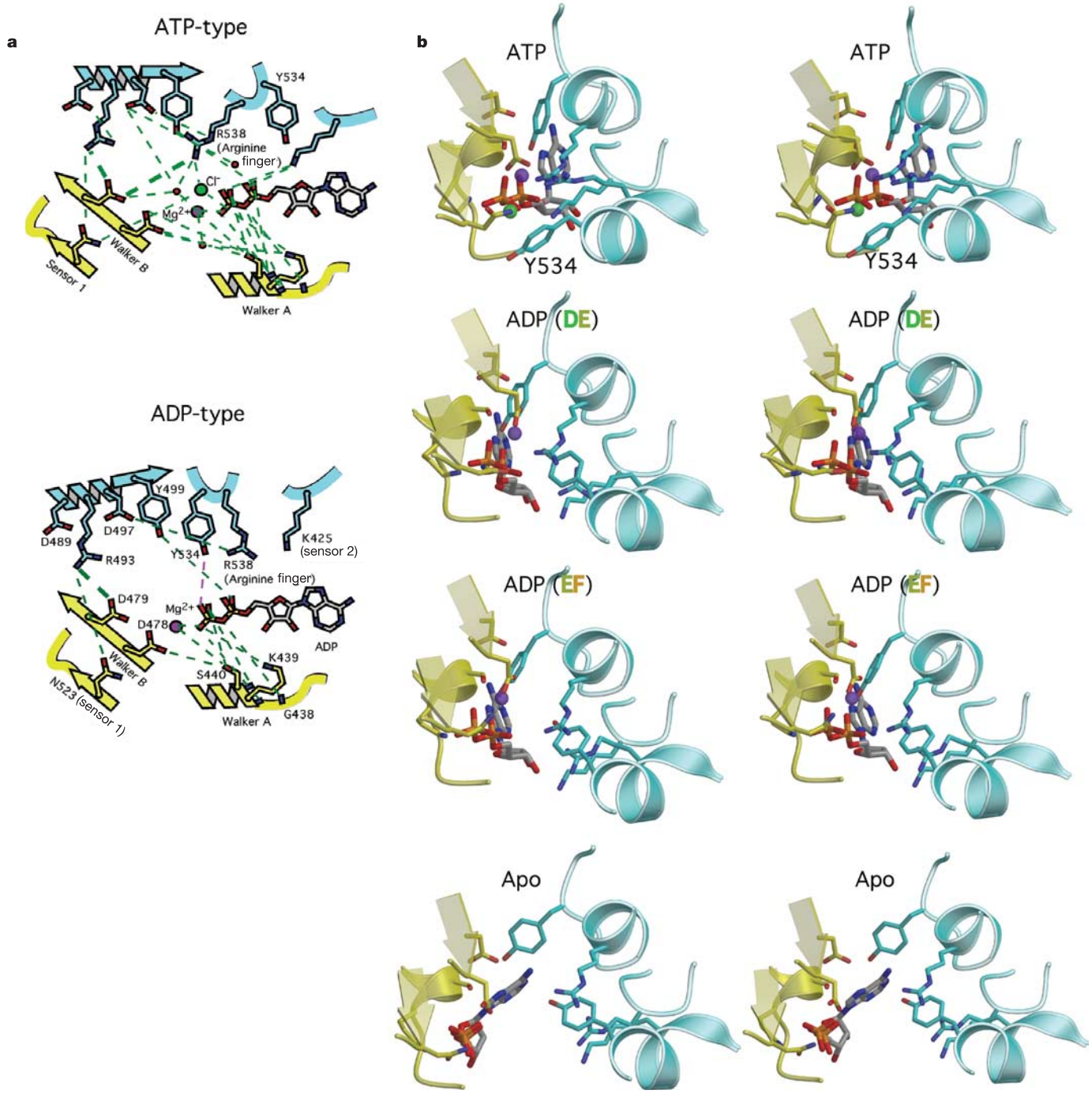

Figure 3 | Intersubunit interactions and nucleotide binding. **a**, **b**, The hydrogen-bonding networks in the intersubunit nucleotide coordination types shown as a schematic (**a**) and in stereoview (**b**). The subunit containing the Walker A, Walker B and sensor-1 motifs is coloured yellow; the adjacent subunit containing the arginine finger is coloured cyan. Mg^{2+} ions are coloured purple and Cl^- ions are green. The ATP-like coordination (top) has multiple interactions and engages R538 and K425. A Cl^- ion is generally observed at the anticipated position for a γ-PO_4. The ADP-like configuration has fewer interactions, and the position of Y534 between R494 and R538 precludes the interactions observed in the ATP-like case. K425 is too distant to interact with the nucleotide. Successive ADP-type configurations (middle) show increasing separation between the subunits. The apo configuration is shown at the bottom.

arranged with a 1 nucleotide per subunit increment. As a result, a straightforward and compelling DNA translocation mechanism integrating these details can be inferred (Fig. 4). Each DNA-binding hairpin maintains continuous contact with one unique nucleotide of ssDNA and migrates downward via ATP hydrolysis and subsequent ADP release at the subunit interfaces. ATP hydrolysis occurs between subunits located towards the top of the staircase, while ADP release occurs between subunits located towards the bottom. The downward movements of the hairpins are coordinated by the staircasing interactions described above. The hairpin at the bottom of the staircase releases its associated ssDNA phosphate to conclude its journey through the hexameric channel. Upon binding a new ATP molecule, this subunit moves to the top of the staircase to pick up the next available ssDNA phosphate, initiating its escorted journey through the channel and repeating the process. For one full cycle of the hexamer, each subunit hydrolyses 1 ATP molecule, releases 1 ADP molecule and translocates 1 nucleotide through the interior channel. A full cycle, therefore, translocates 6 nucleotides with associated hydrolysis of 6 ATPs and release of 6 ADPs.

Both hexamers display a noticeable gap between the AAA+ domains located at the top and bottom positions of the staircase (Fig. 1b). This interface is where the most sizeable movements occur in the mechanism proposed here. Upon ATP binding, the subunit at the bottom of the staircase moves to the top position and closes this gap. Simultaneously, a new gap opens between this subunit and the previous subunit (now bottom). The two hexamers in the crystal display different configurations at this interface, as demonstrated by the different number of ATP-like (and empty) states and the number of hairpins engaged in ssDNA coordination (Supplementary Table S1). For hexamer 1, an ATP-type configuration is observed between subunits A and B, but the hairpin of subunit A is not engaged in ssDNA coordination. Subunit A is consistent with a subunit that has recently bound an ATP molecule, but has not yet bound DNA (see also Fig. 2b, c). This state is not present in hexamer 2, where the subunit at the top of the staircase has an ATP state and binds to ssDNA. Hexamer 2, however, displays two empty nucleotide states whereas hexamer 1 has only one. Subunit L is the lowest on the hexamer 2 staircase and has no counterpart in hexamer 1. It represents the state that directly precedes ATP binding. This is the only subunit in the structure where no ADP is observed at the P-loop, and it displays much larger thermal parameters in the AAA+ domain than the other subunits.

This mechanism has some similarities to the previously proposed operation of T7gp4. For the previous T7gp4 proposal, successive loops also bind to successive nucleotides but pass them through the channel by handing them off from one loop to the next in a "bucket brigade" manner[26]. In such a mechanism, the loops would maintain a nearly fixed height as the individual nucleotides are passed downward from one loop to the next. In contrast, in the escort mechanism proposed here, each hairpin maintains a continuous set of interactions with one nucleotide, and the entire unit collectively migrates downward. We suggest that the T7gp4 hairpins also co-migrate with a given nucleotide in an analogous coordinated escort mechanism. The assigned nucleotide configurations in the crystal structure of T7gp4 in complex with ADPNP[25] place the DNA-binding loops of the ATP-assigned coordination farthest from the primase domains, while the empty state places them closest, in agreement with the probable translocation of DNA towards the primase domains.

For T7gp4, subunits engaged in ATP coordination display a higher affinity for DNA than the ADP and empty states[27]. The same relative order of affinities in the E1 hexamer would lead to an additional driving force for the coordinated escort mechanism of cyclic DNA translocation because subunits at the top of the staircase would have a higher affinity for DNA (more prone to bind) than those at the bottom of the staircase (more prone to release). Binding of a new ATP molecule by a subunit in the empty state at the bottom of the staircase would serve not only to return it to the top of the staircase, but also to increase its affinity for DNA.

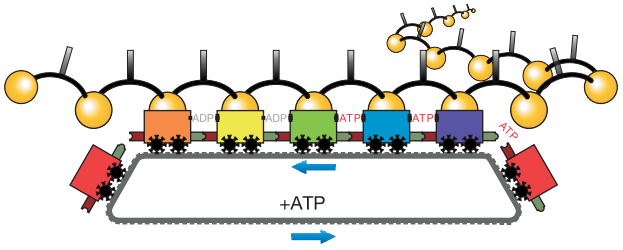

Figure 4 | Cartoon depiction of a coordinated escort mechanism for the E1 hexameric helicase. Each subunit is depicted as a wagon (or boxcar), colour-coded as in Fig. 1. Each wagon transports one DNA nucleotide from the right side to the left. Staircasing interactions are depicted by the wagon couplers. ATP hydrolysis and ADP release occur along the path as depicted by the nucleotide coordination type between the wagons. The red, leftmost wagon ejects its associated DNA nucleotide and returns to the right side upon binding a new ATP molecule. This wagon then picks up the next DNA nucleotide of the series, couples to the purple wagon, and carries its cargo towards the left. Figure prepared by J. Duffy.

Translocation direction

The mechanism described here directly couples ATP hydrolysis to DNA translocation by using ATP hydrolysis to drive the sequential movement of the hairpins and pump ssDNA in that direction. This mechanism is consistent with the demonstrated $3' \rightarrow 5'$ polarity for SF3 helicases and the observed polarity of the DNA in the structure with the $5'$ end located towards the top (oligomerization domain side) of the complex. Previously, the opposite translocation direction was proposed for Tag[13], where the same correlation of hairpin height with nucleotide configuration was identified in the absence of DNA. DNA was proposed to translocate from the empty associated state (bottom) towards the ATP-associated state (top). A drawback of that mechanism is that it does not derive any work from ATP hydrolysis. Such a mechanism is energetically driven by ATP binding. ATP hydrolysis would only serve to facilitate return to the empty state.

Oligomerization domain as processivity factor

The rigid collar formed by the oligomerization domains could serve as a single-stranded equivalent of double-stranded processivity factors such as polymerase sliding clamps like PCNA. Whereas PCNA holds dsDNA topologically together, the static ring formed by six oligomerization domains in the E1 helicase keeps two strands topologically apart. This function would be important to prevent the ring from falling off the substrate DNA because the AAA+ domains have relatively weak interactions between the subunits, including a significant gap between the subunits with the bottom and top hairpins. The robust intersubunit interactions of the ring formed by the oligomerization domains ensure that the hexamer continues to surround the given single strand.

Final remarks

A translocation mechanism in which ATP is hydrolysed sequentially from one subunit to the next with the staircase migrating downward may constitute a general mechanism for hexameric helicases. Although the three nucleotide-binding configurations observed in the structure define relative positions for the ATP, ADP and empty states in a coordinated escort mechanism, the precise details regarding the sequence and timing of ATP hydrolysis, phosphate release, ADP release and ATP binding in this mechanism remain to be determined. This mechanism might not operate by one exclusive timing of these events; slight variations might operate in parallel as described for T7gp4 (ref. 28). The localization of the double-stranded/single-stranded fork junction in this complex also remains

unclear. This species may involve the DBD, which in this model is anticipated to be proximal to the dsDNA entering the complex.

The assembly of the helicase at the *ori* relies upon the DBD. The ultimate helicase species established at the *ori* is a double hexamer[29]. Our structure suggests that the double hexamer consists of two individual hexamers that encircle opposing single strands. The helicase activity of this species results from unidirectional translocation along the encircled strand with steric exclusion of the other, as described for other helicases such as the RNA helicase NPH-II[30]. The mechanism described here can be used to establish two different species where the hexamers remain associated or move apart, as seen by electron microscopy[31,32] (see Supplementary Fig. S5). Further studies are necessary to address these issues.

METHODS

Complex preparation. A fragment encoding BPV-1 E1 residues 306–577 was generated by polymerase chain reaction (PCR) amplification from an expression plasmid template provided by A. Stenlund, and cloned into pGEX-4T-1 (Amersham). The GST fusion protein was expressed in *E. coli* and purified in a manner analogous to methods described previously for other E1 GST fusion proteins[15], and was concentrated in the presence of 5 mM ADP and 200 mM $MgCl_2$.

Crystallization and data collection. The sample was mixed with excess oligo-dT oligonucleotide (13-mer), and immediately used for crystallization trials. Crystals grew at 17 °C by the hanging-drop method with a well solution consisting of 100 mM KCl. Crystals were flash frozen in a stream of cold nitrogen gas (100 K) at beamline X26C of the NSLS for evaluation of diffraction. The most favourable sample was transferred to liquid nitrogen and moved to beamline X29 for data collection. Data collection statistics are shown in Supplementary Table S2.

Structure determination and refinement. The structure was solved by molecular replacement with the program PHASER[33] by placing 12 copies of a hybrid search model consisting of the previously reported helicase domain of HPV-18 E1 (ref. 24) (Protein Data Bank code 1TUE) and the helicase domain of BPV E1 (E.J.E., T. J. Takara, A. Stenlund and L.J., unpublished structure of E1(368–577) refined to 1.65 Å). Further details on the data collection, structure determination and refinement can be found in Supplementary Information.

Received 8 April; accepted 1 June 2006.

1. Messer, W. The bacterial replication initiator DnaA. DnaA and oriC, the bacterial mode to initiate DNA replication. *FEMS Microbiol. Rev.* **26,** 355–374 (2002).
2. Bell, S. P. & Dutta, A. DNA replication in eukaryotic cells. *Annu. Rev. Biochem.* **71,** 333–374 (2002).
3. Hickman, A. B. & Dyda, F. Binding and unwinding: SF3 viral helicases. *Curr. Opin. Struct. Biol.* **15,** 77–85 (2005).
4. Neuwald, A. F., Aravind, L., Spouge, J. L. & Koonin, E. V. AAA+: A class of chaperone-like ATPases associated with the assembly, operation, and disassembly of protein complexes. *Genome Res.* **9,** 27–43 (1999).
5. Seo, Y. S., Muller, F., Lusky, M. & Hurwitz, J. Bovine papillomavirus (BPV) encoded E1 protein contains multiple activities required for BPV DNA replication. *Proc. Natl Acad. Sci. USA* **90,** 702–706 (1993).
6. Yang, L. *et al.* The E1 protein of the papillomavirus BPV-1 is an ATP dependent DNA helicase. *Proc. Natl Acad. Sci. USA* **90,** 5086–5090 (1993).
7. Sedman, J. & Stenlund, A. The papillomavirus E1 protein forms a DNA-dependent hexameric complex with ATPase and DNA helicase activities. *J. Virol.* **72,** 6893–6897 (1998).
8. Ahnert, P. & Patel, S. S. Asymmetric interactions of hexameric bacteriophage T7 DNA helicase with the 5′- and 3′-tails of the forked DNA substrate. *J. Biol. Chem.* **272,** 32267–32273 (1997).
9. LeBowitz, J. H. & McMacken, R. The *Escherichia coli* dnaB replication protein is a DNA helicase. *J. Biol. Chem.* **261,** 4738–4748 (1986).
10. Egelman, E. H., Yu, X., Wild, R., Hingorani, M. M. & Patel, S. S. Bacteriophage T7 helicase/primase proteins form rings around single-stranded DNA that suggest a general structure for hexameric helicases. *Proc. Natl Acad. Sci. USA* **92,** 3869–3873 (1995).
11. Kaplan, D. L. & O'Donnell, M. DnaB drives DNA branch migration and dislodges proteins while encircling two DNA strands. *Mol. Cell* **10,** 647–657 (2002).
12. Seo, Y. S. & Hurwitz, J. Isolation of helicase alpha, a DNA helicase from HeLa cells stimulated by a fork structure and signal-stranded DNA-binding proteins. *J. Biol. Chem.* **268,** 10282–10295 (1993).
13. Gai, D., Zhao, R., Li, D., Finkielstein, C. V. & Chen, X. S. Mechanisms of conformational change for a replicative hexameric helicase of SV40 large tumor antigen. *Cell* **119,** 47–60 (2004).
14. Li, D. *et al.* Structure of the replicative helicase of the oncoprotein SV40 large tumour antigen. *Nature* **423,** 512–518 (2003).
15. Enemark, E. J., Chen, G., Vaughn, D. E., Stenlund, A. & Joshua-Tor, L. Crystal structure of the DNA binding domain of the replication initiation protein E1 from papillomavirus. *Mol. Cell* **6,** 149–158 (2000).
16. Luo, X., Sanford, D. G., Bullock, P. A. & Bachovchin, W. W. Solution structure of the origin DNA-binding domain of SV40 T-antigen. *Nature Struct. Biol.* **3,** 1034–1039 (1996).
17. Davey, M. J. & O'Donnell, M. Replicative helicase loaders: ring breakers and ring makers. *Curr. Biol.* **13,** R594–R596 (2003).
18. Jeruzalmi, D., O'Donnell, M. & Kuriyan, J. Clamp loaders and sliding clamps. *Curr. Opin. Struct. Biol.* **12,** 217–224 (2002).
19. Enemark, E. J., Stenlund, A. & Joshua-Tor, L. Crystal structures of two intermediates in the assembly of the papillomavirus replication initiation complex. *EMBO J.* **21,** 1487–1496 (2002).
20. Gillette, T. G., Lusky, M. & Borowiec, J. A. Induction of structural changes in the bovine papillomavirus type 1 origin of replication by the viral E1 and E2 proteins. *Proc. Natl Acad. Sci. USA* **91,** 8846–8850 (1994).
21. Sanders, C. M. & Stenlund, A. Recruitment and loading of the E1 initiator protein: an ATP-dependent process catalysed by a transcription factor. *EMBO J.* **17,** 7044–7055 (1998).
22. Schuck, S. & Stenlund, A. Assembly of a double hexameric helicase. *Mol. Cell* **20,** 377–389 (2005).
23. Chen, G. & Stenlund, A. Sequential and ordered assembly of E1 initiator complexes on the papillomavirus origin of DNA replication generates progressive structural changes related to melting. *Mol. Cell. Biol.* **22,** 7712–7720 (2002).
24. Abbate, E. A., Berger, J. M. & Botchan, M. R. The X-ray structure of the papillomavirus helicase in complex with its molecular matchmaker E2. *Genes Dev.* **18,** 1981–1996 (2004).
25. Singleton, M. R., Sawaya, M. R., Ellenberger, T. & Wigley, D. B. Crystal structure of T7 gene 4 ring helicase indicates a mechanism for sequential hydrolysis of nucleotides. *Cell* **101,** 589–600 (2000).
26. Crampton, D. J., Mukherjee, S. & Richardson, C. C. DNA-induced switch from independent to sequential dTTP hydrolysis in the bacteriophage T7 DNA helicase. *Mol. Cell* **21,** 165–174 (2006).
27. Hingorani, M. M. & Patel, S. S. Interactions of bacteriophage T7 primase/helicase protein with single-stranded and double-stranded DNAs. *Biochemistry* **32,** 12478–12487 (1993).
28. Liao, J. C., Jeong, Y. J., Kim, D. E., Patel, S. S. & Oster, G. Mechanochemistry of t7 DNA helicase. *J. Mol. Biol.* **350,** 452–475 (2005).
29. Fouts, E. T., Yu, X., Egelman, E. H. & Botchan, M. R. Biochemical and electron microscopic image analysis of the hexameric E1 helicase. *J. Biol. Chem.* **274,** 4447–4458 (1999).
30. Kawaoka, J., Jankowsky, E. & Pyle, A. M. Backbone tracking by the SF2 helicase NPH-II. *Nature Struct. Mol. Biol.* **11,** 526–530 (2004).
31. Wessel, R., Schweizer, J. & Stahl, H. Simian virus 40 T-antigen DNA helicase is a hexamer which forms a binary complex during bidirectional unwinding from the viral origin of DNA replication. *J. Virol.* **66,** 804–815 (1992).
32. Lin, B. Y., Makhov, A. M., Griffith, J. D., Broker, T. R. & Chow, L. T. Chaperone proteins abrogate inhibition of the human papillomavirus (HPV) E1 replicative helicase by the HPV E2 protein. *Mol. Cell. Biol.* **22,** 6592–6604 (2002).
33. McCoy, A. J., Grosse-Kunstleve, R. W., Storoni, L. C. & Read, R. J. Likelihood-enhanced fast translation functions. *Acta Crystallogr. D* **61,** 458–464 (2005).
34. Esnouf, R. M. An extensively modified version of MolScript that includes greatly enhanced coloring capabilities. *J. Mol. Graph.* **15,** 132–134 (1997).
35. Bacon, D. J. & Anderson, W. F. A fast algorithm for rendering space-filling molecule pictures. *J. Mol. Graph.* **6,** 219–220 (1988).
36. Merritt, E. A. & Murphy, M. E. P. Raster3D version 2.0 - A program for photorealistic molecular graphics. *Acta Crystallogr. D* **50,** 869–873 (1994).

Supplementary Information is linked to the online version of the paper at www.nature.com/nature.

Acknowledgements We thank H. Robinson (beamline X29) and A. Héroux (beamline X26C) for support with data collection at the National Synchrotron Light Source (NSLS) at Brookhaven National Laboratory. We also thank G. Hannon and A. Gann for critical reading of the manuscript, and B. Stillman, N. Tolia and members of the Joshua-Tor laboratory for discussions. The NSLS is supported by the US Department of Energy, Division of Materials Sciences and Division of Chemical Sciences. This work was supported by an NIH grant to L.J.

Author Information Coordinates and structure factors are deposited in the Protein Data Bank under accession code 2GXA. Reprints and permissions information is available at npg.nature.com/reprintsandpermissions. The authors declare no competing financial interests. Correspondence and requests for materials should be addressed to L.J. (leemor@cshl.edu).